Diyala Journal of Engineering Sciences

Journal homepage: https://djes.info/index.php/djes

ISSN: 1999-8716 (Print); 2616-6909 (Online)

# Influence of Interpass Welding Temperature on the Microstructure and Mechanical Properties of Super Duplex Stainless Steel AISI 2507

Mohammed Helan Sar[1*], Sara H. Shahatha[2], Sami Chatti[3], Mondher Zidi[3]

[1] Department of Applied Mechanics Techniques Engineering, Engineering Technical College, Middle Technical University, Baghdad, Iraq
[2] Department of Materials Techniques Engineering, Engineering Technical College, Middle Technical University, Baghdad, Iraq
[3] Laboratory of Mechanical Engineering, National Engineering School of Monastir, University of Monastir, Tunisia

**ARTICLE INFO**

**Article history:**
Received: 05/09/2025.
Revised: 28/05/2026.
Accepted: 31/05/2026.
Available online: 15/06/2026.

**Keywords:**
Stainless steel AISI2507
ER2209
GTAW
Cooling rate
Temperature
Multipass welding

**ABSTRACT**

*This study investigates the combined influence of interpass temperature and cooling rate on the microstructure and mechanical properties of 10-mmthick AISI 2507 superduplex stainless steel welded by multi-pass gas tungsten arc welding (GTAW) using ER2209 filler metal. Welded joints were produced under controlled thermal conditions to evaluate the effect of welding thermal cycles on phase evolution and hardness distribution. Optical microscopy, X-ray diffraction (XRD), and Vickers microhardness testing were employed to characterize the weld metal (WM), heat-affected zone (HAZ), and base metal (BM). The results demonstrated that cooling rate was the dominant parameter governing microstructural evolution. Rapid cooling promoted the formation of a finer duplex microstructure with a more homogeneous ferrite–austenite distribution, whereas slower cooling resulted in grain coarsening and increased ferrite retention at grain boundaries. The investigated interpass temperature range (150–350°C) had only a limited influence on the mechanical response, with the weld metal hardness remaining nearly constant at approximately 288–289 HV, indicating that the ferrite–austenite balance was effectively maintained under the selected welding conditions. XRD analysis confirmed the preservation of the duplex structure through the characteristic ferrite (α) (110) and (200) and austenite (γ) (111) and (200) diffraction peaks in all welded samples. However, the slower-cooling condition exhibited higher ferrite peak intensities, suggesting reduced austenite reformation during solidification. The combined microstructural, XRD, and hardness results demonstrate that the cooling rate exerts a greater influence than the interpass temperature on phase stability, microstructural refinement, and the overall metallurgical performance of multi-pass GTAW AISI 2507.*

## 1. INTRODUCTION

Duplex stainless steels consist predominantly of two phases: ferrite (BCC) and austenite (FCC). The mutually dependent nature of their volumes provides duplex stainless steel with a combination of mechanical strength and corrosion resistance unmatched by other alloys. Duplex stainless steels, when annealed in a solution-annealed condition, will generally have almost equal amounts of both phases. However, maintaining at least this amount of phase balance is very important for retaining high-quality performance throughout the lifetime of these materials [1, 2]. Compared to typical austenitic stainless steel (SS), duplex SS has approximately twice the yield strength and excellent resistance to chloride pitting, crevice corrosion, and stress corrosion cracking; therefore, duplex steels exhibit excellent durability in corrosive service environments [3, 4]. Among these materials is super duplex SS AISI 2507, which has enhanced resistance to corrosive environments because AISI 2507 has increased levels of chromium, molybdenum, and nitrogen compared to other duplex SS alloys. These properties can be retained after welding when suitable heat input and thermal control are applied during fabrication [5, 6].

Fusion welding disrupts the ferrite–austenite phase balance in duplex stainless steels due to the thermal cycles of melting and solidification, which may adversely affect corrosion resistance and toughness [7,8]. Appropriate control of welding parameters and post-weld thermal treatment can promote phase rebalancing, minimize undesirable microstructural changes, and restore the mechanical and corrosion performance of welded joints [9,10]. When compared to each of its two distinct phases, DSSs are frequently more powerful. The yield strengths of the duplex grades are twice as high as those of the typical austenitic grades, and they maintain excellent ductility throughout

* Corresponding author's E-mail: mheilan14@yahoo.com
DOI: 10.24237/djes.2026.19212

the procedure [11]. The thermal history during welding plays a significant role in controlling phase transformation and microstructural evolution in duplex stainless steels. In particular, interpass temperature influences cooling conditions, which, in turn, affect the ferrite–austenite balance and the development of the weld microstructure [12,13]. As a result, the interpass temperature and heat input should be carefully controlled to maintain the desirable duplex structure and ensure that welded joints meet acceptable mechanical and corrosion performance standards [14-16].

Duplex stainless steels contain approximately 20%-25% chromium and 2%-7% nickel and offer an excellent balance of mechanical strength and corrosion resistance, with lower nickel content than traditional austenitic stainless steels, providing better cost stability [17, 18]. Molybdenum and nitrogen, which are interpreted or modified as alloying elements present in duplex stainless steels, enhance the resistance to pitting and crevice corrosion, stabilize the ferrite-austenite phase balance, and inhibit the formation of detrimental intermetallic phases during thermal processing and welding (i.e., by nitrogen) [19, 20]. Nitrogen provides additional strengthening to the duplex stainless steel [6]. In several grades of duplex stainless steel, manganese is substituting for nickel to increase nitrogen solubility while retaining the desired duplex phase balance. Grades 2101 and 2304 of duplex stainless steel are classified as lean duplex stainless steels according to their chemical composition. Grade 2205 is typically referred to as a 22Cr duplex, and grades 2507 (UNS S32750) and 4501 are considered 25Cr super duplex stainless steels [21, 22]. Duplex stainless steels exhibit magnetic behavior due to the presence of the ferritic phase, which differs from that of a completely austenitic stainless steel [23, 24].

The solidification of duplex stainless steels begins with ferrite formation, followed by partial conversion to austenite during cooling. The amount of ferrite-to-austenite transformation is governed mostly by the alloy's composition and the cooling conditions, thereby directly affecting the final ferrite-austenite balance and resulting microstructure [25,26]. The weldability of duplex stainless steels is strongly influenced by the chemical composition of both the base and filler metals, as well as by welding parameters such as heat input and cooling conditions. Appropriate control of these variables is essential to preserve phase balance, suppress detrimental phase formation, and achieve the required mechanical and corrosion performance [27,28]. To achieve high-quality multi-pass welds, maintain a stable weld metal microstructure and promote adequate austenite reformation within the heat-affected zone (HAZ) to preserve the ferrite–austenite balance and ensure satisfactory mechanical and corrosion properties [29, 30]. In addition, apply appropriate thermal control to suppress the precipitation of deleterious intermetallic phases, particularly the sigma (σ) phase, which can significantly impair the performance of duplex stainless steel weldments [31]. Regulating the ferrite-austenite equilibrium in welds is more intricate than in base metals. The beneficial duplex microstructure of these stainless steels is negatively impacted during fusion welding due to melting and solidification processes [20].

Numerous studies have investigated how different welding processes affect the composition, structure, and quality of duplex and superduplex stainless steel. Xavier et al. [32] found that the interpass temperature is an important factor in determining the heating/cooling cycle, phase balance, and microstructure of a welded workpiece. Poulain et al. [33] reported that poor control of interpass temperatures during the processing of superduplex stainless steels can lead to the formation of undesirable secondary microstructural constituents, thereby reducing mechanical performance. Šimeková et al. [34] evaluated laser beam welding of SAF 2507 and found that the weld thermal cycle significantly affects the amounts of ferrite and austenite that form, thereby influencing the welded microstructure and mechanical performance. Kanagaraj et al. [35] compared GTAW and Regulated Metal Deposition (RMD) root-pass welding techniques for duplex stainless steel and demonstrated that the welding process markedly affects the metallurgical characteristics, mechanical behavior, and corrosion resistance of welded joints. Likewise, Tóth et al. [36] reported that appropriate thermal control during electron beam welding produced a balanced duplex microstructure with satisfactory hardness and impact toughness in super duplex stainless steel. Kumar et al. [37] further showed that GTAW thermal cycles influence the microstructure and corrosion behavior of SAF 2507 by promoting coarsening in the weld and heat-affected zones.

Although previous studies have considerably improved understanding of the metallurgy of duplex and superduplex stainless steels, limited attention has been devoted to the combined influence of cooling rate and interpass temperature during multi-pass GTAW welding of 10 mm-thick AISI 2507 using ER2209 filler metal. Furthermore, few studies have correlated optical microstructural observations with X-ray diffraction (XRD) analysis and hardness measurements under controlled thermal conditions to provide a comprehensive assessment of weld performance. Therefore, the present study investigates the combined effect of interpass temperature and cooling rate on the microstructural evolution and mechanical behavior of multi-pass GTAW welded AISI 2507.

The main contribution of this work is the integrated evaluation of phase evolution, microstructural characteristics, and hardness response using complementary optical microscopy, XRD, and Vickers microhardness analyses. The findings provide practical guidance for optimizing thermal control during welding to preserve phase balance, suppress undesirable phase

precipitation, and improve the metallurgical integrity of super duplex stainless steel welded joints.

## 2. MATERIALS AND METHODOLOGY

This study involved welding dissimilar metals, specifically super duplex stainless steel AISI 2507, utilizing the GTAW technique with a filler metal: ER 2209.

### *2.1 Chemical Composition of Base Metals*

The chemical composition of the used material, AISI 2507, and filler metal 2209 has been tested and matched with the nominal values, as shown in Table 1. The used device is a PMI (Positive Material Identification) brand OLYMPUS portable device.

**Table 1**. Chemical composition of AISI 2507, wt.%

| Element | C% | Si% | Ni% | Cr% | P% | S% | Mo% | Mn% | N% | Cu% | Fe% |
|---|---|---|---|---|---|---|---|---|---|---|---|
| AISI 2507 Nominal | 00.3 | 0.8 | 6.0-8.0 | 24.0-26.0 | 0.035 | 0.020 | 3.0-5.0 | 1.2 | 0.24-0.32 | 0.5 | Bal |
| Actual | 0.013 | 0.38 | 6.91 | 25.17 | 0.026 | 0.001 | 3.80 | 0.86 | 0.27 | 0.29 | Bal |
| ER2209 Nominal | 0.03 | 0.09 | 7.5-9.5 | 21.5-23.5 | 0.03 | 0.03 | 2.5-3.5 | 0.5-2.0 | 0.08-0.2 | 0.75 | Bal |
| ER2209 Actual | 0.021 | 0.81 | 8.7 | 23.09 | 0.016 | 0.019 | 3.07 | 1.62 | 0.11 | 0.71 | Bal |

### *2.2 Welding Procedure*

Two varieties of plates, each measuring 20 x 50 cm, were prepared with bevels along the 50 cm edge. For the welding process, a copper backing strip (50 x 10 x 1 cm) was utilized. Key objectives during welding included maintaining a proper cooling rate, preventing slow cooling cycles, and ensuring uniform heat distribution within the welding zone. The actual interpass temperatures investigated were 150 °C and 350 °C. The value of 90 °C referred to a measured condition during preliminary welding. Specific procedural parameters and observations included:

1. The maximum interpass temperature recorded was 90 °C.
2. A shielding gas flow rate of 12–18 liters per minute was maintained, with an 8 mm aperture nozzle size recommended.
3. The heat input for the second pass was reduced by 25% compared to the first pass.
4. The back-weld technique was employed, eliminating the need for a separate purging procedure.
5. During the welding process, upon cessation, the welding current was progressively reduced via remote control. It was critical to maintain the torch over the weld pool until complete solidification and sufficient atmospheric shielding were achieved.
6. A three-second gas pre-flow was initiated before the commencement of each pass or at any stop-start point.
7. The primary variable between the two samples was the inter-pass cooling rate.

The selected interpass temperatures (150℃ and 350 ℃) were chosen based on recommendations from industrial welding guidelines such as NORSOK M-601 and IMOA which recommend controlling the interpass temperature to prevent excessive ferrite retention and harmful phase precipitation. The joint design is represented in Figure 1 and shows the bevel configuration used for full penetration welding. Figure 2 shows the fit-up process along with copper backing strip and plate preparation. The GTAW welding set up and equipment is illustrated in Figure 3.

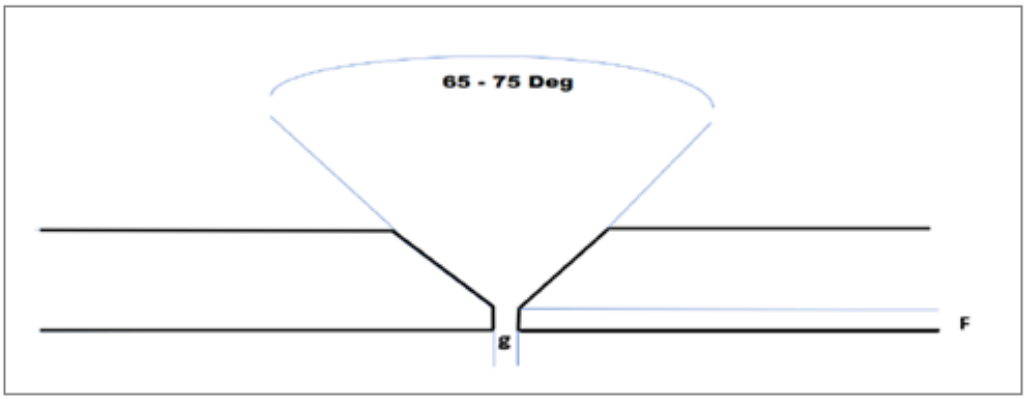


**Figure 1.** Sketch of join design.

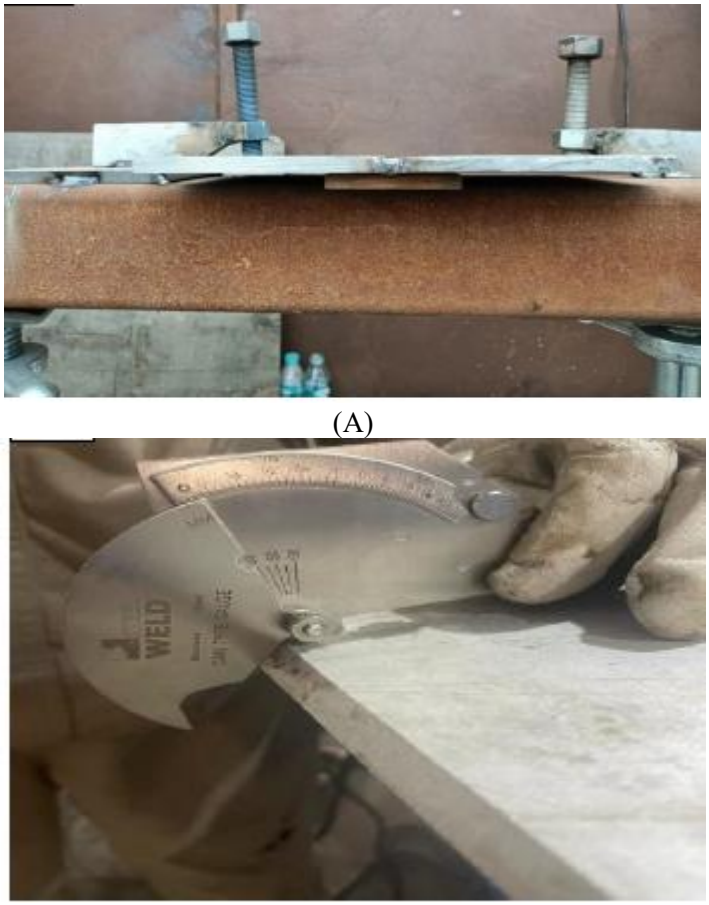


(A)

(B)

**Figure 2.** Fit-up and welding preparation (A) Back strip and mechanical fixtures (B) Stainless steel plate beveling.


**Figure 3.** Welding machine.

*2.3 Non-Destructive Tests (NDT) Visual Inspection*

Visual inspection (VT) was conducted as the initial non-destructive examination to assess the quality of the welded joints before proceeding with destructive and microstructural evaluations. The inspection was performed throughout the welding process and after the completion of all welding passes by a certified welding inspector in accordance with the applicable visual inspection procedures for welded joints. The inspection focused on identifying visible surface imperfections, including surface cracks, undercut, overlap, incomplete fusion, excessive reinforcement, porosity, spatter, arc strikes, and surface oxidation. In addition, the overall weld bead appearance, dimensional consistency, weld profile, alignment of the welded plates, and the degree of angular and longitudinal distortion were carefully examined. Particular attention was paid to ensuring complete weld continuity and the absence of visible discontinuities that could affect subsequent mechanical and metallurgical characterization.

The visual examination confirmed that the welded specimens had a sound surface appearance, with no observable defects exceeding the acceptable quality limits. Consequently, the welded coupons were considered suitable for subsequent microhardness measurements, microstructural characterization, and X-ray diffraction (XRD) analysis. Figure 4 illustrates the visual inspection process carried out by the certified welding inspector.


**Figure 4.** The welding inspector.

*2.4 Mechanical Tests (Micro-hardness)*

The microhardness distribution across the welded joints was evaluated using the Vickers microhardness test to assess the influence of welding thermal cycles on the mechanical response of the base metal (BM), heat-

affected zone (HAZ), and weld metal (WM). The measurements were performed at the Advanced Materials Laboratory, Middle Technical University, using a Shimadzu HMV-G Series (Japan) Vickers microhardness tester under a load of 300 g (HV0.3) with a dwell time of 15 s, in accordance with ASTM E92 (Figure 5). Prior to testing, the welded specimens were sectioned transverse to the welding direction, mechanically ground, and polished to obtain a smooth surface suitable for hardness measurements. Indentations were made along the mid-thickness of the welded cross-section at 1 mm intervals, starting from the base metal on one side, passing through the heat-affected zone and weld metal, and continuing to the opposite side of the joint, as illustrated in Figure 6. This measurement path enabled correlation of the hardness profile with the corresponding microstructural regions affected by the welding thermal cycle. The obtained hardness values were used to evaluate the influence of interpass temperature and cooling rate on the mechanical characteristics of the welded joints and to support the interpretation of the optical microscopy and X-ray diffraction (XRD) results.

**Figure 5.** Micro-hardness device

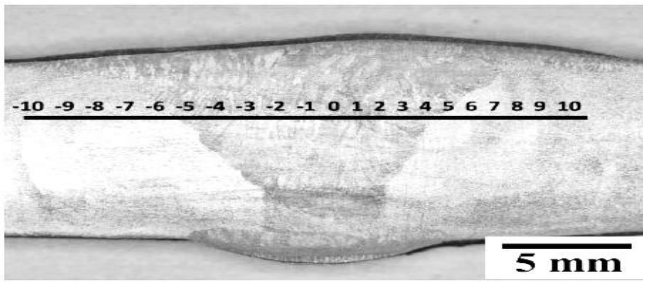


**Figure 6.** Micro-hardness sketch and map

*2.5 Microstructure Tests*

*2.5.1 Specimen Preparation and Microstructural Analysis*

The specimen fabrication was performed utilizing a wire-cutting apparatus. Subsequent preparation involved cold mounting, followed by sequential grinding with varying grades of ASTM emery papers (320, 400, 600, 800, 1000, 1200, and 1500). The polishing procedures used specialized cloths, as well as different sizes (0.05 µm and 3 µm). After polishing, the samples were polished with water and an alcohol solution, then dried to yield a reflective surface.

The microstructure of the sample was evaluated by viewing cross-sections of the base and weld metal from various types of welding processes using an optical microscope, "MEIJI", and an associated camera for Super Duplex Stainless Steel (Figure 7). Sample preparation included grinding, polishing, and etching. The etching process used a mixture of 3 parts HCl, 2 parts HNO3, and 2 parts acetic acid. The macrostructural examination identified the fusion line, heat-affected zone, and any macro-fracture.


**Figure 7.** Microstructure device

*2.5.2 XRD Diffractometer*

To determine the different crystalline phases present in weld metal produced with ER2209 filler material and to evaluate how thermal conditions during welding will impact those phases (and/or their stability), the welding metallurgical analysis was conducted via X-ray Diffraction (XRD). A SHIMADZU XRD-6000 diffractometer (manufactured in Japan) was used to complete the XRD analysis. The operating voltage of the XRD is 40 kV, and it utilized Cu Kα radiation (λ = 1.5406 Å), as shown in Figure 8. The XRD diffractograms produced by the diffraction patterns of the sample were used to identify the following two crystalline phases: α-BCC (i.e., ferrite) and γ-FCC (i.e., austenite). Furthermore, analysis of the diffractograms identified potential undesirable secondary phase formations that may lead to reduced mechanical properties and/or reduced corrosion resistance in the

weld joints. Qualitative comparison of the XRD data for each sample (generated under different welding conditions) enabled assessment of the influence of cooling rate and interpass temperature on phase evolution and the occurrence of ferrite-austenite balance. Results from the XRD analysis were subsequently compared with optical microstructure analyses and Vickers microhardness tests to provide a comprehensive evaluation of the metallurgical behavior of the weld joints.

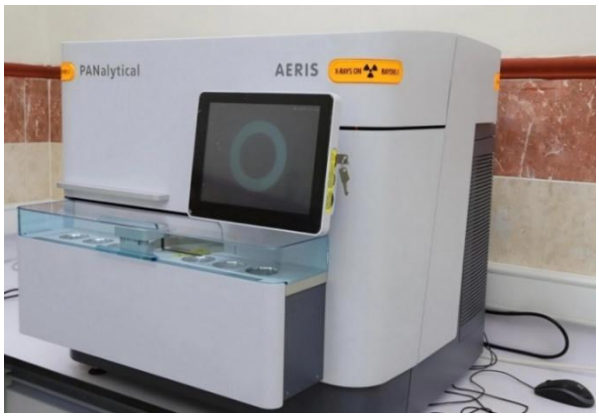


**Figure 8.** XRD device

## 3. RESULTS AND DISCUSSION

### *3.1 Hardness Test*

Vickers microhardness profiles measured over the base metal (BM), heat-affected zone (HAZ), and weld metal (WM) are shown in Figure 9. The hardness values were largely consistent across the welded joints, with about 288 - 289 HV recorded for the weld metal under the measured welding parameters. All specimens had similar hardness, regardless of the interpass temperature used during welding, suggesting that the thermal environment did not significantly affect the mechanical properties of the weld metal. The consistent hardness distribution can be attributed to the maintenance of phase balance between ferrite and austenite, and to minimal formation of secondary phases, which would have negatively impacted the phase balance between the two dominant phases in this family of duplex stainless steels. According to Gunn [38], hardness relates closely to phase balance (particularly phase content) and the formation of intermetallic compounds. Since the phase constitution of the welds did not change with the different interpass temperatures, hardness remained nearly unaffected across the entire weld region. Slight local variations were observed within the heat-affected zone and weld metal and can be associated with differences in thermal exposure during successive welding passes and the resulting microstructural heterogeneity. However, these variations were limited and did not indicate localized hardening or softening that could adversely affect joint integrity. The obtained hardness profiles are consistent with the optical microscopy and XRD results, which confirmed retention of the duplex microstructure under both cooling conditions. These findings indicate that, within the investigated thermal range, cooling conditions primarily influenced microstructural refinement rather than producing measurable hardness changes.

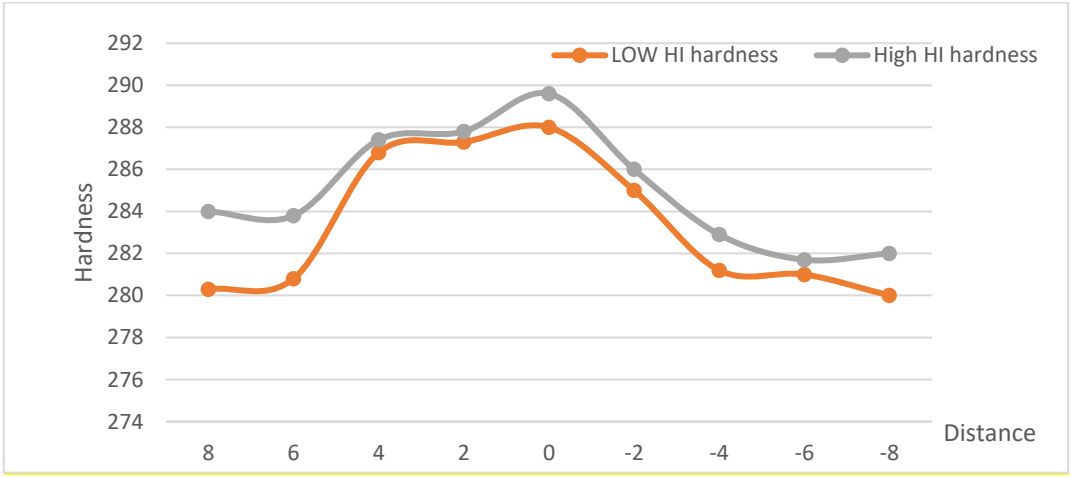


**Figure 9.** Comparison between the hardness of two samples.

### *3.2 Microstructure Properties (Optical Analysis)*

The BM possesses a microstructure characteristic of wrought duplex stainless steels, consisting of ferrite and austenite phases (Figure 10). The dark region represents the ferrite phase, whereas the austenite phase is illustrated as the white region. The island-like austenite phase is embedded in the continuous ferrite matrix and stretched along the rolling direction. On the AISI 2507 side, the BM contains equiaxed austenite grains, as shown in Figure 10. The observed microstructures show that a faster cooling rate leads to the formation of a finer austenite in the ferritic matrix whereas a slower cooling rate leads to grain growth and formation of more grain-boundary precipitates. This behavior is consistent with diffusion-controlled phase transformation mechanisms, in which slower cooling promotes reformation of austenite, but may also encourage harmful phases, such as chromium carbides [5], as shown in Figure 11. The optical micrographs and XRD patterns qualitatively confirmed the retention of

the duplex microstructure in the weld metal under both of the cooling conditions. However, quantitative determination of ferrite and austenite phase fractions was beyond the scope of the present study. Therefore, future work should involve the quantitative phase analysis through image analysis, Feritscope measurements, or EBSD to better evaluate the phase balance in the weld metal and heat-affected zone.

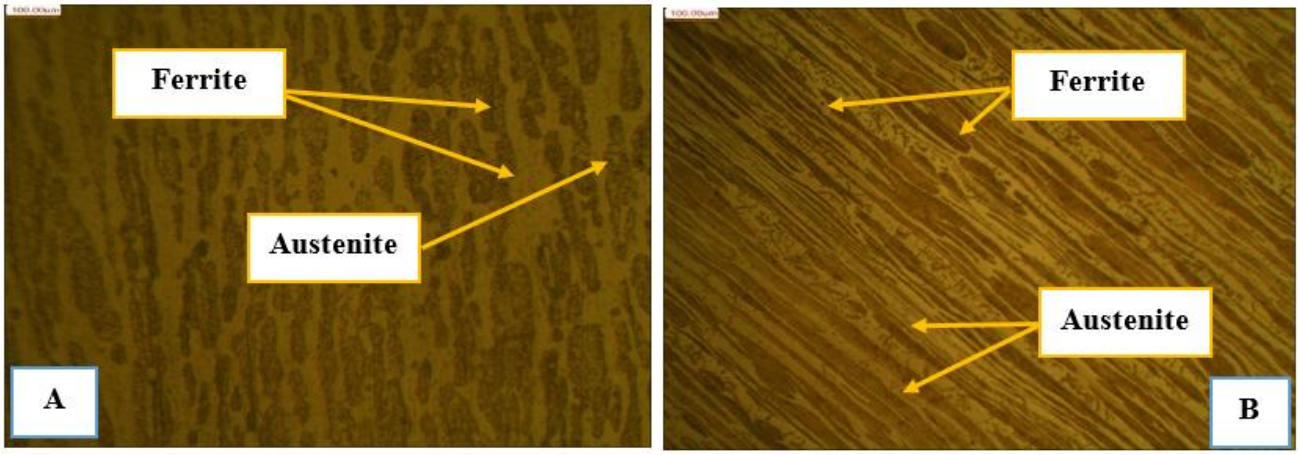


**Figure 10.** The microstructure of weld metals: A. High cooling rate and B. slow cooling rate of inter-pass temperature.

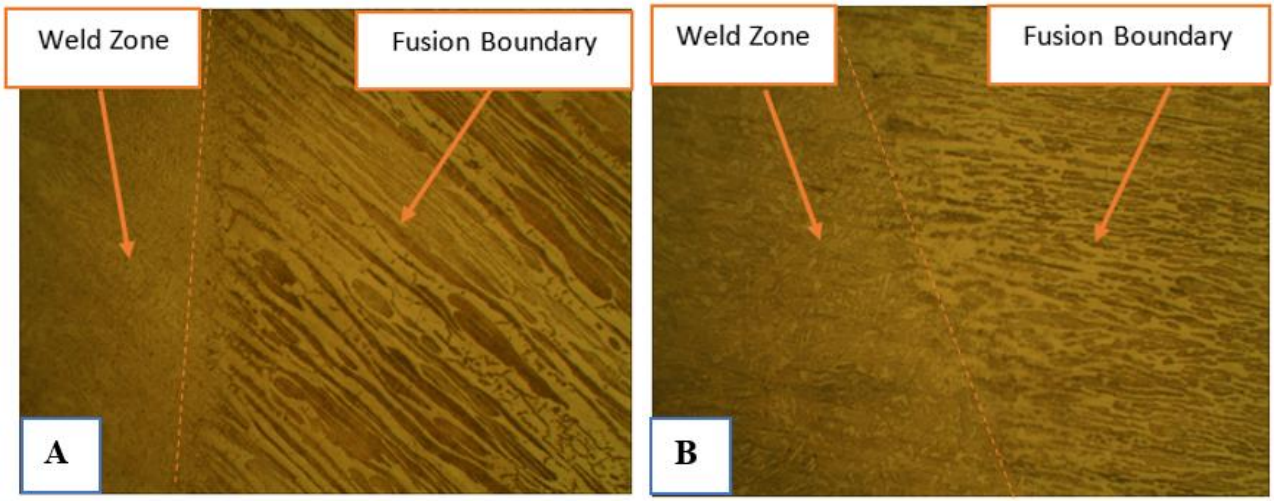


**Figure 11.** Optical micrographs of HAZs, A. High cooling rate and B. slow cooling rate of inter-pass temperature

*3.3 XRD Analysis*

The XRD patterns obtained from the weld metal produced using ER2209 filler metal are presented in Figure 12. The diffraction results confirmed the presence of the two characteristic phases of duplex stainless steel, namely ferrite (α, BCC) and austenite (γ, FCC), indicating that the duplex microstructure was successfully retained after the multi-pass GTAW process. Both examined cooling conditions yielded principal diffraction peaks for ferrite ((110) and (200)) and austenite ((111) and (200)).

Further comparison of diffraction patterns indicated that the raw material cooled slowly exhibited higher intensity (I) values at ferrite peaks than the rapidly cooled raw material. This suggests that, due to decreased diffusion kinetics and a limited amount of austenite reformation during cooling, more ferrite may have been retained in raw materials subjected to slow cools than in those subjected to rapid cools. On the other hand, rapid cooling produced a more even (i.e., ferrite-austenite) phase distribution, which supports the presence of fine duplex microstructures, as seen in the optical micrographs. Although a quantitative phase-fraction analysis was not conducted, differences in intensities of diffraction peaks provide qualitative evidence for the effect of cooling conditions on phase evolution, consistent with the known transformation behavior of duplex stainless steels [39].

Additionally, no intermetallic phase diffraction peaks were observed within the XRD detection limits, suggesting that the welding parameters were adequate to retain the duplex phase constitution. Finally, the XRD data support the nearly constant hardness values (approximately 288–289 HV) observed at different interpass temperatures. This indicates that, within the investigated thermal range, interpass temperature had only a limited effect on the ferrite–austenite balance, whereas cooling rate played the dominant role in controlling microstructural evolution. Therefore, effective

cooling control is a key factor for maintaining phase stability and ensuring the metallurgical integrity of multi-pass GTAW-welded AISI 2507 super duplex stainless steel.

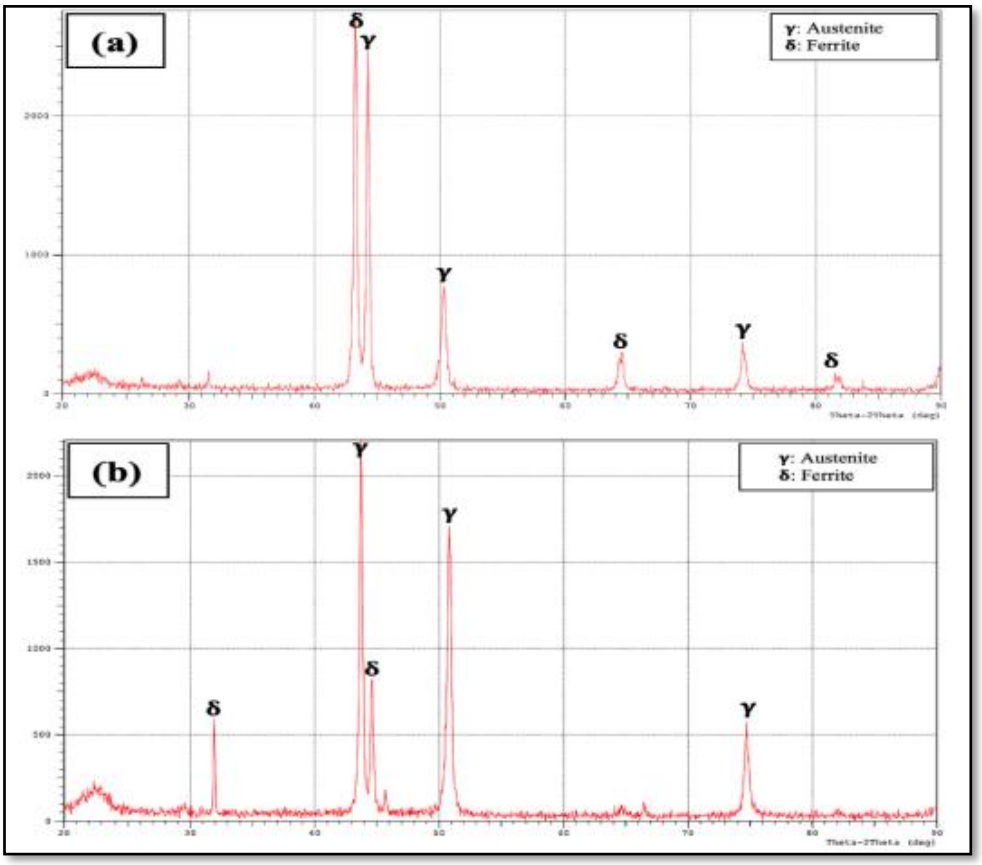


**Figure 12.** XRD analysis of WMs produced with ER2209, A. High cooling rate and B. slow cooling rate of inter-pass temperature

## 4. CONCLUSION

The effects of cooling rate and interpass temperature on the welding behavior of AISI 2507 super duplex stainless steel were examined via microstructural analysis and experimental investigation in this study. The experimental results provided valuable insight into the thermal response, phase stability, and hardness characteristics of the welded joints as functions of the thermal conditions under which they were manufactured. The conclusions drawn in this investigation are as follows:

- Within the interpass temperature range of 150–350 °C, there was limited effect on the measured hardness of the welded joints. Hardness values remained fairly constant (approximately 288–289 HV).
- The rate of cooling significantly affected the microstructural characteristics of the weld metal. Faster cooling produced a fine duplex structure, whereas slower cooling led to grain coarsening and precipitate formation at grain boundaries.
- X-ray diffraction (XRD) analysis confirmed that ferrite and austenite phases were present and stable in each welded sample; therefore, the duplex microstructure was preserved after the GTAW process.
- Weld samples that cooled more slowly had a greater intensity of the ferrite peak, indicating less reformed austenite during solidification and cooling.
- Based on these findings, it can be concluded that controlling the cooling conditions during welding is important for providing microstructural stability and improving the overall mechanical and metallurgical properties of AISI 2507 super duplex stainless steel weldments.

## REFERENCES

[1] K. W. Chan and S. C. Tjong, “Effect of secondary phase precipitation on the corrosion behavior of duplex stainless steels,” Materials, vol. 7, no. 7, pp. 5268–5304, 2014, doi: 10.3390/ma7075268.

[2] A. K. Maurya, C. Pandey, and R. Chhibber, “Dissimilar welding of duplex stainless steel with Ni alloys: A review,” International Journal of Pressure Vessels and Piping, vol. 192, Art. no. 104439, 2021, doi: 10.1016/j.ijpvp.2021.104439.

[3] H. Wang, A. Wang, C. Li, X. Yu, J. Xie, and C. Liu, “Effect of secondary-phase precipitation on mechanical properties and corrosion resistance of 00Cr27Ni7Mo5N hyper-duplex

stainless steel during solution treatment," Materials, vol. 15, no. 21, Art. no. 7533, 2022, doi: 10.3390/ma15217533.
[4] Y. Peng, Y. Du, Y. Zhang, W. Ma, and Q. Liang, "Effect of solution treatment on microstructure and mechanical properties of laser-cladded Stellite 6 coatings on 2507 duplex stainless steel," Materials Today Communications, vol. 46, Art. no. 112795, 2025, doi: 10.1016/j.mtcomm.2025.112795.
[5] L. Chen, H. Tan, Z. Wang, J. Li, and Y. Jiang, "Influence of cooling rate on microstructure evolution and pitting corrosion resistance in the simulated heat-affected zone of 2304 duplex stainless steels," Corrosion Science, vol. 58, pp. 168–174, 2012, https://doi.org/10.1016/j.corsci.2012.01.018.
[6] G. Chagas de Souza et al., "Mechanical properties and corrosion resistance evaluation of superduplex stainless steel UNS S32760 repaired by GTAW process," Welding International, vol. 30, no. 6, pp. 432–442, 2016, doi: 10.1080/09507116.2015.1096527.
[7] O. S. Barrak, S. Ben-Elechi, and S. Chatti, "Parameters influence on mechanical properties of resistance spot welding: AISI304L/AISI1005," Pollack Periodica, vol. 20, no. 1, pp. 102–109, 2025, doi: 10.1556/606.2024.01142.
[8] Y. Yang, N. Patil, S. Askar, and A. Kumar, "Machine learning-guided study of residual stress, distortion, and peak temperature in stainless steel laser welding," Applied Physics A, vol. 131, Art. no. 44, 2025, doi: 10.1007/s00339-024-08145-8.
[9] M. Zhang, Y. Lu, S. Chen, L. Rong, and H. Lu, "Effect of dilution ratio of the first 309L cladding layer on the microstructure and mechanical properties of weld joint of connecting pipe-nozzle to safe-end in nuclear power plant," Acta Metallurgica Sinica, vol. 56, no. 8, pp. 1057–1066, 2020, doi: 10.11900/0412.1961.2019.00449.
[10] M. A. Valiente Bermejo, D. Eyzop, K. Hurtig, and L. Karlsson, "Welding of large thickness super duplex stainless steel: Microstructure and properties," Metals, vol. 11, no. 8, Art. no. 1184, 2021, doi: 10.3390/met11081184.
[11] A. Di Schino, "Manufacturing and applications of stainless steels," Metals, vol. 10, no. 3, Art. no. 327, 2020, doi: 10.3390/met10030327.
[12] F. A. A. Macedo et al., "Influence of the interpass welding temperature on microstructure and corrosion resistance of superduplex stainless steel SAF 2507," Materials Research, vol. 24, no. 3, 2021, https://doi.org/10.1590/1980-5373-MR-2020-0239.
[13] A. Higelin, S. Le Manchet, G. Passot, et al., "Heat-affected zone ferrite content control of a duplex stainless steel grade to enhance weldability," Welding in the World, vol. 66, no. 8, pp. 1503–1519, 2022, doi: 10.1007/s40194-022-01326-0.
[14] P. Bellamkonda, M. Dwivedy, M. Sudersanan, et al., "Influence of welding processes on the microstructure and mechanical properties of duplex stainless steel parts fabricated by wire arc additive manufacturing," Metals and Materials International, vol. 31, pp. 368–391, 2025, doi: 10.1007/s12540-024-01753-2.
[15] A. H. Abbood, M. H. Sir, and N. S. M. Namer, "Corrosion behavior in different media of dissimilar super duplex stainless steel 2507 and austenitic stainless steel 316 welding by using GTAW process with filler type 316L," Journal of Techniques, vol. 5, no. 3, pp. 185–193, 2023, doi: 10.51173/jt.v5i3.1103.
[16] M. Maslak, M. Stankiewicz, and B. Ślazak, "Duplex steels used in building structures and their resistance to chloride corrosion," Materials, vol. 14, no. 19, Art. no. 5666, 2021, doi: 10.3390/ma14195666.
[17] A. S. Fedorov and A. I. Zhitenev, "Duplex stainless steels: Requirements, challenges, and solutions," Metallurgist, vol. 68, pp. 1809–1818, 2025, doi: 10.1007/s11015-025-01894-8.
[18] L. Karlsson, "Welding duplex stainless steels—A review of current recommendations," Welding in the World, vol. 56, no. 5–6, pp. 65–76, 2012, doi: 10.1007/BF03321351.
[19] B. H. Lee et al., "Intergranular corrosion characteristics of super duplex stainless steel at various interpass temperatures," International Journal of Electrochemical Science, vol. 10, pp. 7535–7545, 2015, https://doi.org/10.1016/S1452-3981(23)17369-X.
[20] P. Paulraj and R. Garg, "Effect of intermetallic phases on corrosion behavior and mechanical properties of duplex stainless steel and super-duplex stainless steel," Advances in Science and Technology Research Journal, vol. 9, pp. 87–105, 2015, doi: 10.12913/22998624/59090.
[21] V. D. Cojocaru, M. L. Angelescu, N. Șerban, N. Zărnescu-Ivan, and E. M. Cojocaru, "Effects of solution treatment on the microstructure and mechanical properties of UNS S32750/F53/1.4410 SDSS alloy," Materials, vol. 18, no. 23, Art. no. 5447, 2025, doi: 10.3390/ma18235447.
[22] C. R. Xavier et al., "An experimental and numerical approach for the welding effects on the duplex stainless steel microstructure," Materials Research, 2015, https://doi.org/10.1590/1516-1439.302014.
[23] D. Vysochinskiy and D. Rybakov, "On the effect of various heat treatments on microstructure of AISI 4130 steel used in sour service pipes," in Proceedings of the ASME 2020 39th International Conference on Ocean, Offshore and Arctic Engineering (OMAE2020), vol. 3, Materials Technology, Virtual Conference, Aug. 3–7, 2020, Paper V003T03A008, doi: 10.1115/OMAE2020-18017.
[24] L. Pezzato and I. Calliari, "Advances in duplex stainless steels," Materials, vol. 15, no. 20, Art. no. 7132, 2022, doi: 10.3390/ma15207132.
[25] J. A. Castro et al., "Effects of local heat input conditions on the thermophysical properties of super duplex stainless steels," Materials Research, 2018, https://doi.org/10.1590/1980-5373-MR-2017-0384.
[26] H. Sieurin and R. Sandström, "Sigma phase precipitation in duplex stainless steel 2205," Materials Science and Engineering: A, vol. 444, no. 1–2, pp. 271–276, 2007, https://doi.org/10.1016/j.msea.2006.08.107.
[27] C. Örnek, M. G. Burke, T. Hashimoto, and D. L. Engelberg, "748 K (475 °C) embrittlement of duplex stainless steel: Effect on microstructure and fracture behavior," Metallurgical and Materials Transactions A, vol. 48, no. 4, pp. 1653–1665, 2017, doi: 10.1007/s11661-016-3944-2.
[28] O. S. Barrak, H. Ben Slama, S. Ben-Elechi, and S. Chatti, "Resistance spot welding of dissimilar metals (AISI 1005 and AISI 304L): Experimental and numerical investigation of tensile-shear and vibration loads," Journal of Techniques, vol. 7, no. 4, pp. 53–67, 2025, doi: 10.51173/jt.v7i4.2776.
[29] H. Tan, Y. Jiang, B. Deng, T. Sun, J. Xu, and J. Li, "Effect of annealing temperature on the pitting corrosion resistance of super duplex stainless steel UNS S32750," Materials Characterization, vol. 60, no. 9, pp. 1049–1054, 2009, https://doi.org/10.1016/j.matchar.2009.04.009.
[30] H. Hemmer and Ø. Grong, "A process model for the heat-affected zone microstructure evolution in duplex stainless steel weldments: Part I. The model," Metallurgical and Materials Transactions A, vol. 30, no. 11, pp. 2915–2929, 1999. https://doi.org/10.1007/s11661-999-0129-2.
[31] P. Ferro and F. Bonollo, "A semiempirical model for sigma-phase precipitation in duplex and superduplex stainless steels," Metallurgical and Materials Transactions A, vol. 43, pp. 1109–1116, 2012. https://doi.org/10.1007/s11661-011-0966-7.
[32] C. R. Xavier et al., "Numerical prediction for the effects of welding interpass temperature on the thermal history and microstructure of duplex stainless steels," Materials Research, vol. 26, 2023, https://doi.org/10.1590/1980-5373-MR-2022-0529.

[33] P. Poulain, J. Wang, S. Bouvier, S. Williams, S. Budnyk, and A. Gavrilovic-Wohlmuther, "Impact of interpass temperature on the microstructure and mechanical properties of super duplex stainless steel in CW-GMA additive manufacturing," Journal of Manufacturing Processes, vol. 146, pp. 30–43, 2025, doi: 10.1016/j.jmapro.2025.04.091.

[34] B. Šimeková et al., "Microstructural and mechanical characterization of the laser beam welded SAF 2507 super-duplex stainless steel," Metals, vol. 14, no. 10, Art. no. 1184, 2024, doi: 10.3390/met14101184.

[35] P. Kanagaraj, B. Visvalingam, V. Varadhan, and K. Radhakrishnan, "Influence of root pass welding techniques (GTAW and RMD) on metallurgical, mechanical and corrosion behaviour of gas metal arc welded duplex stainless-steel plates," Canadian Metallurgical Quarterly, pp. 1–27, 2026, doi: 10.1080/00084433.2026.2659551.

[36] T. Tóth, A. C. Hesse, V. Kárpáti et al., "Microstructural and mechanical properties of electron beam welded super duplex stainless steel," Welding in the World, vol. 68, pp. 1929–1940, 2024, doi: 10.1007/s40194-024-01680-1.

[37] S. Kumar, Y. Kumar, and K. E. K. Vimal, "Microstructural and corrosion behavior of thin sheet of stainless steel-grade super duplex 2507 by gas tungsten arc welding," SAE International Journal of Materials and Manufacturing, 2024, doi: 10.4271/05-17-02-0011.

[38] R. N. Gunn, Duplex Stainless Steels: Microstructure, Properties and Applications. Cambridge, U.K.: Woodhead Publishing, 1997.

[39] A. H. M. Saeed et al., "Welding tantalum by resistance spot welding with metal plating interlayer," AIP Conference Proceedings, vol. 3105, 2024, https://doi.org/10.1063/5.0212440.